



# Effect Of Stirrup Shape On The Torsional Behavior Of RC Girders And Frames.

<sup>1</sup>Mohamed Fathy, <sup>2</sup>Mahmoud Lasheen, <sup>3</sup>Ayman Hussein

<sup>1</sup> B.Sc. Degree, Civil Engineering, <sup>2</sup> Assistant Professor of Structural Engineering, <sup>3</sup> Professor of Structural Engineering

<sup>1</sup>Department of Structural Engineering,

<sup>1</sup>Ain Shams University, Cairo, Egypt

**Abstract:** This study examines the impact of various methods for reinforcing concrete beams on their capacity to resist twisting forces. Rather than using only traditional closed-loop stirrups. The test program was divided into three beams: conventional closed, two-piece, and U-shaped stirrups that can be assembled in situ. Using a specialized testing machine, they compared these alternative designs with conventional stirrups to see which performed better under pure twisting loads. Measuring how much twisting force each could handle, how flexible they were, and how stiff they remained under load. The outcomes presented significant observations: beams with two-piece stirrups performed about the same as traditional ones in terms of maximum strength, but beams with U-shaped stirrups had 9% higher torsional strength than conventional designs. U-shaped stirrups showed 10% more ductility than conventional closed ones and were 16% more ductile than two-piece stirrups. The energy dissipation analysis showed that U-shaped stirrups absorbed an average of 1.707 kN·m<sup>2</sup>/rad-significantly more than conventional closed stirrups (1.345 kN·m<sup>2</sup>/rad) and two-piece enclosed stirrups (1.251 kN·m<sup>2</sup>/rad). This means U-shaped stirrups were able to dissipate about 21.3% more energy than closed stirrups and roughly 26.8% than the two-piece design. Comparing the test results against (ACI 318-19 and ECP 203 code) predictions revealed that the code was reasonably close for initial cracking (within 16%), it severely undervalued the ultimate torsional strength by nearly half (47%), and (53%), respectively, especially when non-conventional stirrup configurations were used.

**Index Terms** - RC beams, Pure torsion, Stirrup's Configuration, Ductility, Stiffness.

## I. INTRODUCTION

Buildings, bridges, and other structures that use reinforced concrete beams must be resistant to significant torsional stress. Building standards and specifications provide explicit guidelines for designing structures for torsion using a thin-tube space truss as an example. Torsion-sensitive beams with a homogeneous cross-section can be compared to thin-walled tubes without a concrete core, according to this comparison. Reinforced concrete beams' rotational strength is mostly due to the longitudinal and transverse reinforcements, as well as the concrete's function as compression diagonals. While several researchers investigated stirrup spacing, reinforcement ratios, and spiral configurations, few have systematically examined the effect of stirrup shape on torsional resistance. The performance of (HSC) hollow beams reinforced with steewereooks and basalt fiber polymer (BFP) bars in combined shear, torsion, and moment was examined by MohamedSalih & Yousif (2022) [1]. The diameter of the BFP bars, the steel hook spacing, and the ratio of longitudinal to transverse RFT were the factors. Beams with BFP bars and steel hooks with smaller diameters used at closer spacings produced the best results. Longitudinal BFP bars produced superior results compared to steel hooks. Shatarat et al. (2020) [2] used both welded and unwelded transverse RFT to study the torsional mechanism. The following transverse RFT patterns were used: advanced spiral shape, rectangular spiral, circular spiral, and separate. When compared to regular hooks, the results showed that the

specimens with continuous circular hooks were more efficient and achieved the highest improvement in peak torsion resistance. Katkhuda et al. (2019) [3] used transverse RFT to study the torsional mechanism of beams in a variety of shapes, including advanced rectangular spirals, separate, continuous circular and rectangular spirals, and more. According to the findings, using a continuous rectangular spiral increased torsional resistance by 17% more than using individual reinforcement. The effect of reinforcing form and longitudinal and transverse RFT on torsion strength was investigated by Rashidi et al. (2017) [4]. It was discovered that as the reinforcement ratio increased, ductility increased. Both longitudinal and transverse bars are necessary for good torsional behavior in RC beams, and it has been found that they cannot increase the torsional strength of RC beams alone. The torsion test of beams with web holes was investigated by Abdel-Kareem et al. (2020) [5]. Fifteen beams were inspected: eight had reinforcement built around the aperture, six had no reinforcement around the entrance, and one solid beam had no opening. The results demonstrated that adding inclined stirrups at a 45-degree angle to the longitudinal pivot of the samples increased the torque from the solid sample by 90%. The flexural behavior of beams reinforced with compressive steel bars and two-piece stirrups was examined in Lin F, Zhong Q, and Zhang Z 2016 [6]. Likewise, torsional behavior is problematic when it is anticipated that the beams would withstand torsion. The torsional behavior of the beams under discussion may be negatively impacted by three configuration changes between those that use traditional one-piece stirrups and those that use two-piece stirrups with crossties and U-shaped stirrups. In the past, attempts have been made to comprehend how monolithically cast RC beams behave under torsion. Analytical models that fall into two main categories can be used to interpret their torsional behavior: i) the skew bending theory [7], which served as the foundation for the American Code from 1971 to 1995; and ii) the space truss analogy (STA) [8-9], which has served as the foundation for the Chinese code since 1989, the European Model Code since 1978, and the American Code since 1995. The understanding of the torsional behavior of beams has recently increased due to a few experimental and analytical studies [10–12]. These analytical methods, however, did not consider the beam design indicated above, which is connected to two-piece stirrups with crossties and U-shaped stirrups. To address the limited understanding of stirrup shape on torsional behavior, three distinct transverse reinforcement stirrups were used in systematic experimental investigations into the beams' torsional behavior. Three RC beams that had been tested were employed, considering each beam's unique configuration. The design and construction process of a reinforced concrete (RC) girder utilizing these methods is shown in **Fig. 1**. In certain wrapped joint details, the application of reinforcement is limited due to the use of one-piece closed stirrups. The adoption of two-piece stirrups or U-shaped stirrups may address some of these challenges. Thus, the purpose of this work is to investigate how transverse stirrup shape affects the torsional strength, evaluate crack patterns, and recommend optimal stirrup designs for girder applications of RC beams that enhance structural integrity and safety in construction applications.

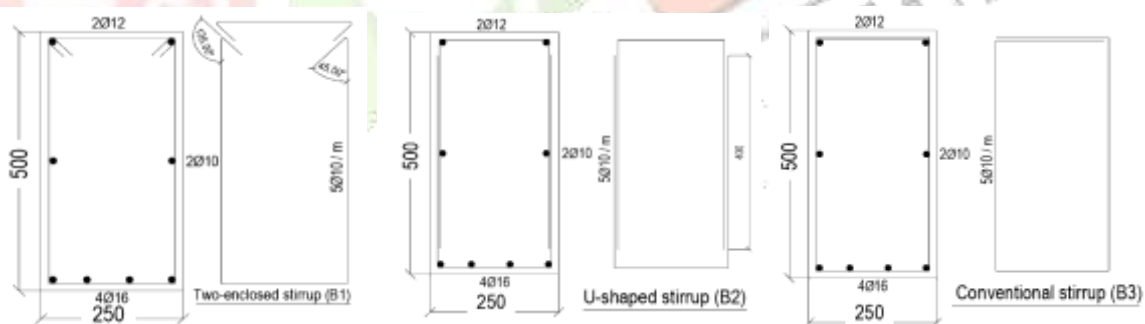


**Fig. 1 Configuration of two-piece stirrup, U-shaped stirrup, and closed stirrup.**

## II. METHODOLOGY

The current study aims to determine how different stirrup shapes affect the torsional behavior of RC beams. Various stirrup configurations were used as transverse reinforcement in the RC beams to identify which had the highest torsional capacity. By testing three RC beams (B1, B2, and B3) with a cross-sectional size of 250 mm × 500 mm, the average compressive strength of the beams is 32 MPa. The theoretical values derived from the ACI318-19 code [13] are compared in this section with the experimental cracking torsional moment ( $T_{cr}$ ) and ultimate torsional moment ( $T_u$ ). Throughout the entire experimental loading process, each specimen was designed to withstand torsional failure, prevent bending, and shear failure.

### III. EXPERIMENTAL PROGRAM

#### 3.1 CHARACTERISTICS OF THE TESTED BEAMS

Three rectangular-cross-sectioned RC beams make up the experimental program in this investigation. Three different forms of transverse reinforcement were used for the beams: two-piece stirrup with crosstie, U-shaped stirrup, and traditional (closed stirrup) as shown in **Fig. 2**. The test group included three cast specimens (B1, B2, and B3) with a cross-sectional size of 250 mm × 500 mm. All the specimens have a consistent length of 4500 mm. All the RC beams were cast using the same concrete mix. The next sections provide the specimen details, test process, concrete mix proportion, concrete mechanical characteristics, and steel mechanical properties.



**Fig. 2 Configuration of two-piece, U-shaped, and closed stirrup on site.**

#### 3.1 CONCRETE MIX PROPORTION AND MECHANICAL PROPERTIES OF USED MATERIAL

The proportion of the concrete mix is shown in **Table 1**. After 28 days of curing, the average compressive strength of the three concrete cubes for each specimen was determined (see **Fig. 3**). The average experimental values for the mechanical characteristics of steel and concrete are presented in **Table 2**, **Table 3**. All measured properties meet or exceed the minimum requirements of the adopted codes, confirming material compliance for structural design under both ultimate and serviceability limit states.

**Table 1: Concrete Mix Proportion.**

1 $\square$ 3	Cement	Coarse Aggregates	Fine Aggregates	Water	Super-plasticizer	Slump
	400 kg	1080 kg	720 kg	180 liters	6 liters	12-15 cm

**Table 2: Detailed Statistical Analysis by Beam.**

Exp. Beam	Individual Cube Strengths (MPa)	Average (MPa)	Modulus of Elasticity (MPa)	Poisson Ratio	Coefficient of Variation (%)
B1	32.6, 31.8, 32.8, 34.0, 31.7, 31.7	32.4	25	0.2	2.79
B2	34.1, 33.0, 31.4, 32.7, 31.4, 31.4	32.3	25	0.2	3.48
B3	32.3, 29.5, 29.8, 31.3, 30.7, 32.4	31.0	25	0.2	3.96
Average overall	Range: 29.5 - 34.1	31.9	25	0.2	3.85

**Table 3: Material Properties of Concrete and RFT.**

Type	Average Compressive Strength	Yield Strength (MPa)	Modulus of Elasticity (MPa)	Poisson Ratio	Coefficient of Variation (%)
concrete	32 MPa	----	25	0.2	3.85
Bars Ø 16	----	560.00	210	0.3	0.225
Bars Ø 12	----	539.30	210	0.3	0.255
Bars Ø 10	----	515.45	210	0.3	0.269





**Fig. 3 Pouring concrete cubes for all specimens.**

### 3.1 TEST SETUP

Using a standard torsional test apparatus, the specimens will be subjected to pure torsion. Every beam is 4500 mm long. To allow the specimen to spin freely throughout the test, the force is applied to a diagonally positioned I-section steel beam that is supported by two steel arms that are fixed at 1250 mm from the ends of each specimen and rest on two roller supports. Between the two steel arms of the specimen, the torsional zone under study is 2000 mm. The load was applied at a rate of "5 kN per minute". The test machine controlled the load applied (load-controlled). **Fig. 4** shows a picture of the real system; **Fig. 5** shows a schematic diagram of the testing setup. Strain gauges for the transverse stirrups, bottom RFT, and longitudinal RFT were installed in the locations illustrated in **Fig. 6**. Six LVDTs were installed: two on the side of the beam to measure the twist angle, two at the bottom of the beam to measure vertical displacement, and two at the steel cantilevers to measure the differential twist angle per one meter as shown in **Fig. 5**.



Roller support

**Fig. 4 Test Set-up.**

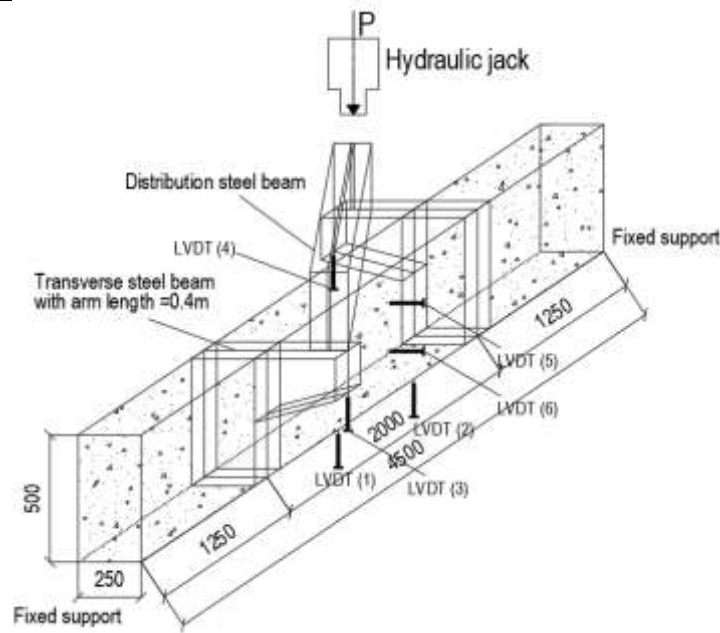


**Fig. 5 Schematic testing rig and instrumentation.**



**Fig. 6 Configuration of strain gauges for the stirrups, bott. RFT, and long RFT.**

## IV. EXPERIMENTAL RESULTS

### 4.1 CRACKING AND FAILURE CHARACTERISTICS

Spiral cracks in each tested beam were indicative of torsional failure. The first crack patterns were the same for all inspected beams. **Fig. 7** illustrates cracks in every beam starting at angles ( $\theta$ ) between 32 and 36 degrees, in addition to the specimens' failure profile. Angle ( $\theta$ ), in the space truss model for torsion, is the angle that the diagonal compressive strut and the longitudinal axis of the beam form. In addition, concrete cover spalling was seen at the corners of each specimen. Spalling off at corners is more likely to occur in specimens with comparatively large stirrup spacing. As the length of these cracks increased, more angled cracks slowly emerged on the two lateral surfaces before extending and joining to create spiral cracks around the circumference of the beam.







**Fig. 7 Failure characteristics and Crack Patterns for tested specimens.**

#### 4.2 TORSIONAL STRENGTH

The experimental cracking torsional moment ( $T_{cr}$ ) and experimental ultimate torsional moment ( $T_u$ ) for each specimen group are shown in **Fig. 8**. The fractures grow and form helical and diagonal cracks on all faces as they spread out from the casting surface. The cracking and ultimate torques were also affected by the stirrups' forms and configuration. Contrasting a beam strengthened with traditional stirrups (B3, specimen) with a reinforced beam with a two-piece stirrup with a crosstie, U-shaped stirrup (B1, B2 example). In comparison to the conventional stirrup (B3, specimen), the U-shaped stirrup-reinforced beam (B2, specimen) showed an average percentage increase of 3% in cracking torques and 9% in ultimate torques. In contrast, the ACI318-19 code [13] forbids the use of U-shaped stirrups that overlap one another to prevent torsion, referencing Behera and Rajagopalan (1969) [14]. The findings show that, in addition to cross-sectional features and concrete strength, the design of the stirrups significantly affects the beams' ability to fracture torsional capacity.

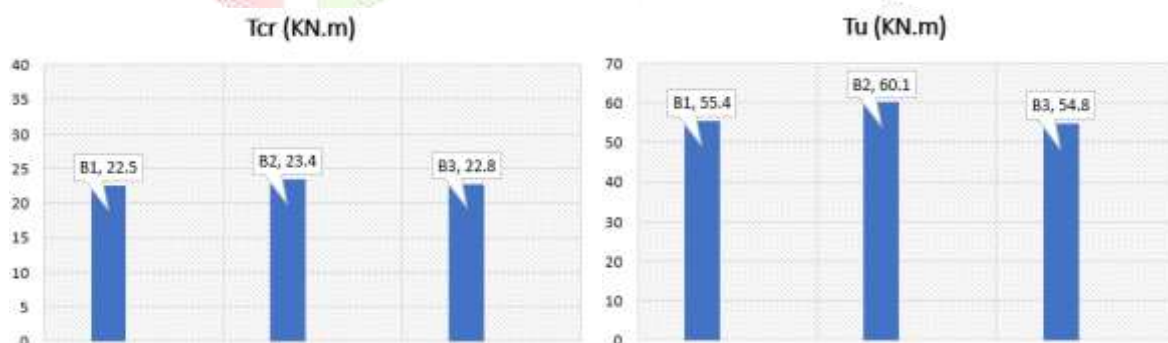


**Fig. 8 Cracking and ultimate torque for experimental specimens.**

#### 4.3 TORQUE - TWIST ANGLE BEHAVIOR

The torque and twisting angles of all tested beams are graphically represented in **Fig. 9**, which confirms that all beams were in an elastic condition, as demonstrated by the linear relationship between torque and twists before cracking. After cracking, the curve becomes nonlinear until it achieves the maximal torque. Three phases could be distinguished in the torsion–twist angle curves: pre-cracked, cracked, and post-cracked. The final torsional strength, yielding, and cracking strengths, along with the matching twist angle in each stage, are shown in **Table 4**. The specimens' results are extremely similar in terms of cracking twist angles,

confirming the elastic stage before cracking. The variation in the yielding stage is roughly 3.5%. In terms of ultimate twist angle, the specimens (B1, B2, B3) equal 0.0354 rad/m, 0.0433 rad/m, and 0.0384 rad/m, respectively. The result of specimen B2 (U-shaped stirrup) has the highest twist angle, by an increase of 11.5%.

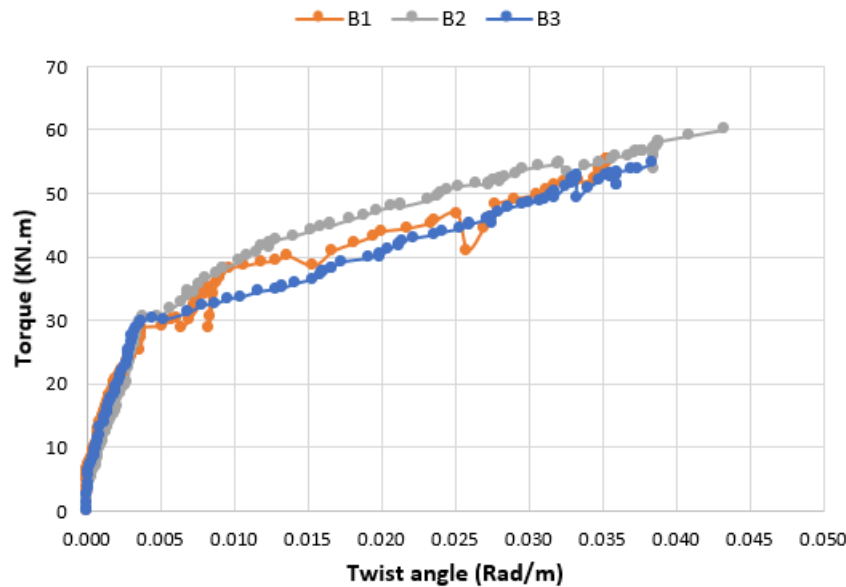


**Fig. 9 Torque versus twist angle for experimental specimens.**

**Table 4: Torsion Strength and Twist angle in the Cracking, Yield, and Ultimate stages.**

Specimen ID	Specimen Dimension	Stirrups Shape	Cracking Stage		Yield Stage		Ultimate Stage	
			Torsion (T <sub>cr</sub> ) (KN.m)	Twist (θ) (Rad/m) x10 <sup>-3</sup>	Torsion (T <sub>y</sub> ) (KN.m)	Twist (θ) (Rad/m) x10 <sup>-3</sup>	Torsion (T <sub>u</sub> ) (KN.m)	Twist (θ) (Rad/m) x10 <sup>-3</sup>
B1	250 x 500	Two-Piece stirrup	22.5	2.72	28.9	3.76	55.4	35.4
B2		U-shaped stirrup	23.5	2.96	30.6	3.88	60.1	43.3
B3		Traditional stirrup	22.8	2.76	29.8	3.79	54.8	38.4

#### 4.4 STRAINS IN TRANSVERSE STIRRUP REINFORCEMENT

The torque-stirrup strain curves for the tested specimens are shown in **Fig. 10**. The specimens behaved similarly. Stirrup strains were modest before the start of concrete cracking, suggesting that the transverse reinforcement was not fully engaged. The stirrup strains increased gradually as breaking occurred, peaking close to the maximum applied torque. According to this pattern, stirrups were not very important in the beginning of cracking but became more important in preventing torsion following cracking. The results also imply that the stirrup shape has a significant impact on improving the torsional response of RC beams during the post-cracking phase. According to the tested beams' relationship between applied torque and transverse stirrup strain, the stirrups attained their yield stress at about 2500  $\mu\epsilon$  with an average torque of B1=29.8, B2=30.2, B3=30.1 KN.m. The transverse stirrups RFT were found to attain the yield stress at a torque that was roughly 53% of the maximum torque. Yielding at 53% of T<sub>u</sub> aligns with the truss analogy and established theory, supporting the reliability of my experimental approach and interpretation.

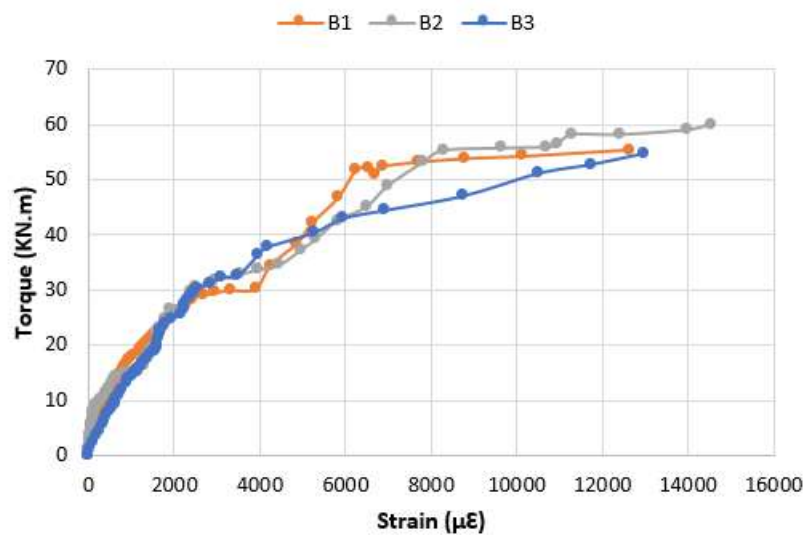


**Fig. 10 Torque - transverse reinforcement strain curves.**

#### 4.5 TORSIONAL DUCTILITY AND ENERGY DISSIPATION

The ability of a structural component to experience significant twisting distortion after reaching its elastic limit is known as torsional ductility. Supporting inelastic rotations under torsional strain, it illustrates the member's resistance to failure. This characteristic is critical for reinforced concrete beams that are subjected to massive or coupled torsional motions, like edge beams, bridge girders, or seismic constructions. A ductility index, which is determined by dividing the ultimate twist angle by the twist angle at yield, is frequently used to represent torsional ductility. An element that has a higher index may be able to withstand more deformation and energy dissipation before failing. The torsional ductility for each experimental specimen is shown in **Table 5**. According to the results of the ductility test, specimen B2 (U-shaped stirrup) is more ductile than B1 (two-enclosed stirrup) and B3 (traditional stirrup) and increases by an average of 16 % and 10 % respectively. The energy dissipation analysis showed that U-shaped stirrups absorbed an average of 1.707 kN·m<sup>2</sup>/rad—significantly more than conventional closed stirrups (1.345 kN·m<sup>2</sup>/rad) and two-piece enclosed stirrups (1.251 kN·m<sup>2</sup>/rad). This means U-shaped stirrups were able to dissipate about 21.3% more energy than closed stirrups and roughly 26.8% more than the two-piece design.

**Table 5: Comparison of torsional ductility for experimental specimens.**

Specimen ID	Specimen Dim.	Stirrups Shape	Torsional ductility		
			Exp. Twist angle at yield point (rad/m) x10 <sup>-3</sup>	Exp. Twist angle at ult. Torque (rad/m) x10 <sup>-3</sup>	Ductility index $\theta_u / \theta_y$
B1	250 x 500	Two-Piece stirrup	3.76	35.4	9.4
B2		U-shaped stirrup	3.88	43.3	11.2
B3		Traditional stirrup	3.79	38.4	10.1

#### 4.6 TORSIONAL STIFFNESS

In the uncracked, elastic phase of loading, a beam's resistance to twisting is known as its initial torsional stiffness. It is often calculated using the first linear segment of the torque-twist response curve, where the material primarily behaves elastically. The stiffness is influenced by the material quality, the cross-sectional shape, and the properties of the uncracked concrete. Currently, the contribution of reinforcement to torsional resistance is relatively minor. As the torsional moment increases and approaches the cracking torque, diagonal fractures begin to form along the section's perimeter. After cracking, the torsional stiffness decreases significantly, leading to a marked reduction in the slope of the torque-twist curve, which indicates the ultimate torsional stiffness. The ultimate torsional capacity during the post-cracking phase. The arrangement and spacing of the stirrups, as well as the interaction between the reinforcement and the nearby cracked concrete,



control it. The longitudinal bars and transverse stirrups that compose a torsional truss mechanism are principally responsible for resisting torsion at this stage, whereas the concrete mostly acts to contain the reinforcement. **Table 6** presents important structural stiffness information by comparing the torsional stiffness of tested beams in the pre-cracking and post-cracking stages. The pre-cracking stage outcomes for each specimen are roughly the same, based on the testing results. While the shape of transverse stirrups has a minor effect on initial torsional stiffness, the B2 (U-shaped stirrup) specimen is less stiff than the other specimens by about 3.5 %. At 90 % of the ultimate load, the U-shaped stirrup specimen decreases in torsion stiffness by about 6.5 %, and the stiffness of all specimens decreased by an average of 87.5 % between the pre-cracking and post-cracking stages.

**Table 6: Comparison of Torsional Stiffness for Experimental Specimens.**

Specimen ID	Specimen Dimension (mm)	Stirrups Shape	Initial torsion stiffness at T 30%			Final torsion stiffness at T 90%			Stiffness drop ratio
			Exp. T <sub>30%</sub> (KN.m)	Exp. twist $\theta_{30\%}$ (rad/m) $\times 10^{-3}$	Stiffness 30% (KN.m <sup>2</sup> )	Exp. T <sub>90%</sub> (KN.m)	Exp. twist $\theta_{90\%}$ (rad/m) $\times 10^{-3}$	Stiffness 90% (KN.m <sup>2</sup> )	
B1	250 X 500	Two-Piece stirrup	16.62	1.302	12765	49.86	30.64	1627	87.3 %
B2		U-shaped stirrup	18.01	1.460	12336	54.02	35.97	1502	87.8 %
B3		Traditional stirrup	16.42	1.324	12402	49.27	31.58	1560	87.4 %

## V. COMPARISON WITH THEORETICAL VALUES

### 5.1 COMPARISON WITH ACI318-19 CODE [13]

This section compares the measured ultimate torsional moment ( $T_u$ ) and cracking torsional moment ( $T_{cr}$ ) with the theoretical values obtained from the ACI318-19 code [13]. The theoretical torsional moment capacity before cracking can be calculated using the following formula:

$$T_{cr} = 0.33 * \sqrt{f_c'} ( [A_{cp}]^2 / P_{cp} ). \quad \text{Eq. (5.1)}$$

Where  $A_{cp}$  is the cross-sectional area of concrete in mm<sup>2</sup>,  $P_{cp}$  is the outside perimeter of a concrete cross-section in mm, and  $f_c'$  is the compressive strength for concrete in MPa. The calculated  $T_{cr}$  Per ACI 318-19 [13] is equal to 19.35 kN.m for specimens (B1, B2, B3). A comparison between the values determined by the ACI code and the experimental cracking torsional moments is shown in **Fig. 11a**. The findings show that the ACI technique is a good reference for design applications since it offers a useful estimate for  $T_{cr}$ . The measured discrepancies ranged from 14.2 % to 17.8 %, with the experimental cracking torsional moments regularly exceeding the ACI estimates. This implies that a safe design margin is provided by the ACI code. The minimum of the following formulas can be used to calculate the theoretical value of the ultimate torsional strength per ACI 318-19:

$$T_{Ac1} = (2 A_o A_v f_{yt} \cot \theta) / S \quad \text{Eq. (5.2)}$$

$$T_{Ac2} = (2 A_o A_s f_y \tan \theta) / (P_h) \quad \text{Eq. (5.3)}$$

Where:  $A_o = 0.85 A_{oh}$ , area enclosed by the path of shear flow around the tube section perimeter (mm<sup>2</sup>),  $A_{oh}$  is the area enclosed by the beam outermost closed stirrup centreline (mm<sup>2</sup>),  $P_h$  is the perimeter of the outermost closed stirrup centreline (mm),  $A_v$  is the area of one-legged steel stirrups in mm<sup>2</sup>,  $f_{yt}$  is the yield strength of the transverse reinforcement in MPa,  $S$  is the spacing of steel transverse reinforcement in mm,  $A_l$  is the area of the total steel longitudinal reinforcement in mm<sup>2</sup>,  $f_y$  is the yield strength of the longitudinal reinforcement

in MPa, and  $\theta$  is the angle of inclination of cracks in degrees. In the space truss analogy, where the longitudinal reinforcement is perpendicular to the transverse reinforcement, the equations mentioned above are based on the longitudinal and transverse reinforcements' respective torsional resisting capacities, disregarding any concrete contribution. The comparison between the experimental ultimate torsional moment and the values determined by the ACI code is shown in **Fig. 11b**. The findings show that a more conservative estimate of  $T_u$  is given by the ACI technique. The experimental ultimate torsional moment consistently exceeded the ACI predictions, the ratios of  $T_{u_{exp}}$  to  $T_{u_{theo}}$  ranging from 1.78 to 1.95. Additionally, it's noted that the U-shaped stirrup (B2 specimen) achieved great torque resistance.

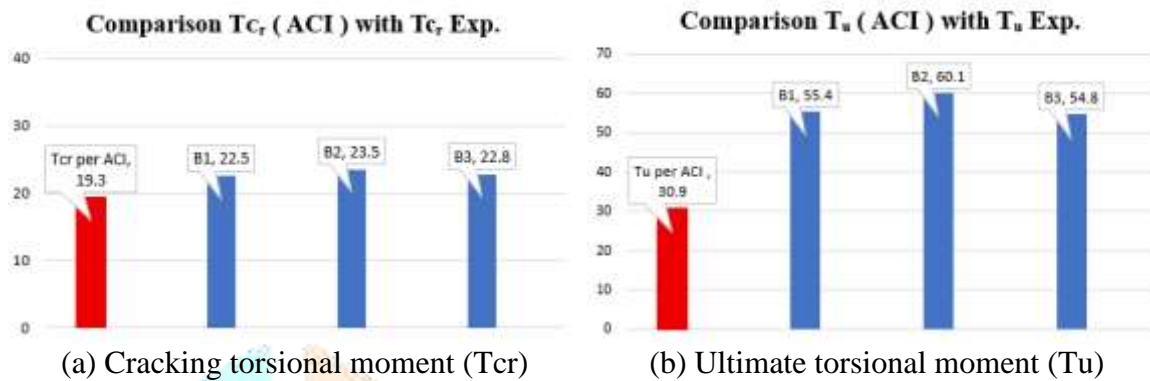


**Fig. 11 Comparison between experimental and theoretical values per the ACI Code**

## 5.2 COMPARISON WITH EGYPTIAN CODE (ECP 203-2020) [15]

This section compares the measured ultimate torsional moment ( $T_u$ ) with the theoretical values obtained from the ECP 203-2020 [15]. The torsional strength is maintained below the minimum shear stress limit,  $q_{u \min}$ , and calculated using Eq. (5.4).  $A_{str}$  is the area of a single branch of the tie stirrup,  $A_{sl}$  is the area of longitudinal reinforcement, where  $b_1$  and  $t_1$  represent the smaller and larger center-to-center dimensions of the closed stirrups, respectively. In the space truss model, the equilibrium's diagonal force is resisted by the concrete compression diagonal. To prevent crushing failure of this compression diagonally, restrictions are applied both on the concrete strut's compressive stresses and on the maximum allowable shear stress. According to the ECP 203 code, resisting torsion is based on the longitudinal and transverse reinforcements' respective torsional resisting capacities, disregarding any concrete contribution. The comparison between the experimental ultimate torsional moment and the values determined by the ECP code is shown in:

$$M_{tu} = \frac{1.7 \cdot b_1 \cdot t_1 \cdot A_{str} \cdot \frac{f_{yst}}{1.15}}{s} \quad \text{Eq. (5.4)}$$

**Fig. 12.** The findings show that a more conservative estimation of  $T_u$  is given by the ECP 203 technique. The experimental ultimate torsional moment consistently exceeded the ECP predictions, the ratios of  $T_{u_{exp}}$  to  $T_{u_{theo}}$  ranging from 2.03 to 2.23. Additionally, it's noted that the U-shaped stirrup (B2 specimen) achieved great torque resistance. The ACI 318-19 [13] and ECP 203 [15] formulae were used to compute the estimated ultimate torsional moments. **Table 7** displays the computed results for each test specimen as well as the torsional moments measured empirically. The findings show that the predictions produced by the ACI and ECP approaches are comparatively close to one another and much conservative. Both design methodologies, however, are generally more cautious and consistently forecast lower torsional capacities in comparison to the actual findings.



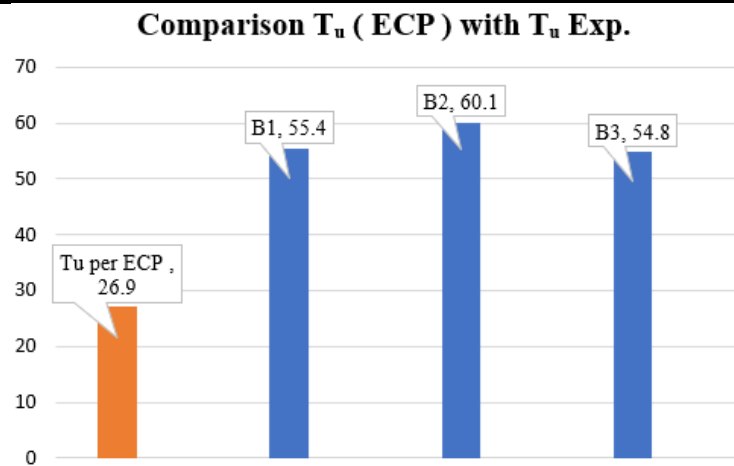


**Fig. 12 Comparison between experimental and theoretical values per the ECP Code**

**Table 7: Summary Comparison of analytical and experimental results.**

Specimen ID	Specimen Dimension (mm)	Stirrups Shape	Ultimate torsion (KN.m)				
			Exp.	ACI	Exp./ACI	ECP	Exp./ECP
B1	250 x 500	Two-piece stirrup	55.4	30.9	1.80	26.9	2.06
B2		U-shaped stirrup	60.1		1.95		2.23
B3		Traditional stirrup	54.8		1.78		2.03

## VI. CONCLUSION

Clarify that study's methodology and findings provide new, specific insights into this issue. For example: "This study fills that gap by systematically evaluating the torsional performance, strength, and ductility of beams with distinct stirrup configurations under pure torsion, using both experimental and analytical approaches. The following deductions are made from the experimental findings and theoretical computations:

1. As control beams, specimens with conventional closed stirrups performed moderately in every parameter tested throughout the test program.
2. Compared to beams with traditional closed stirrups, those reinforced with two enclosed stirrups perform noticeably better under torsional loads. The dual-stirrup design provided useful benefits in construction, especially in crowded joint areas, in addition to improving torsional resistance and crack control.
3. The highest torsional capacity was shown by beams reinforced with U-shaped stirrups, which were on average 9% more torsional than beams with conventional stirrups. In comparison to traditional closed stirrups, the stress distribution of U-shaped stirrups produces a more even distribution of stress around the beam cross-section. Stress concentrations at connecting points are decreased by the continuous steel path in a U-shaped arrangement. Even though U-shaped stirrups lapped together for torsion resistance are not allowed by the ACI 318-19 rule, experimental results indicate that this design has significant practical benefits, particularly in crowded places where conventional reinforcement is challenging to install.
4. U-shaped stirrups are easier to install around longitudinal reinforcement than typical closed stirrups, which need full enclosure. This could improve construction quality and lower installation faults.
5. Ductility results for torsion moment verified that U-shaped stirrups are more effective than conventional closed stirrups at allowing rotational deformation after cracking by an average of 10%

and 16%, respectively, compared to the two-enclosed stirrup. This makes them appropriate for applications that need flexibility under torsional loading or energy dissipation.

6. The average torsional stiffness of beams reinforced with two enclosed stirrups was 6.5% higher than that of U-shaped stirrups and 3.7% higher than that of conventional closed stirrups. Although this arrangement has significant practical benefits, particularly in crowded spaces, it did not surpass U-shaped stirrups in terms of ductility or torsional strength.
7. In all specimens, the initial torsional stiffness was noticeably greater than the post-cracking stiffness, emphasizing the change from uncracked to cracked behavior. Initial torsional stiffness is somewhat impacted by the geometry of transverse stirrups; all specimens' stiffness decreased by an average of 87.5% between the pre-cracking and post-cracking phases.
8. Theoretical predictions based on ACI 318-19 and ECP 203 codes tend to be more conservative when compared to experimental findings. According to ACI provisions, the predicted cracking torsion shows a deviation of approximately 16% below experimental values, while the ultimate torsion is underestimated by around 47%. Similarly, ECP 203 underestimates the ultimate torsional capacity by about 53%. These discrepancies suggest that both codes may not fully account for the enhanced performance provided by non-traditional stirrup configurations. Consequently, current design provisions could benefit from adjustments to better reflect the actual behavior observed in experimental studies.
9. Recommended code enhancements include establishing empirically derived modification factors for varying stirrup configurations, incorporating explicit allowances for U-shaped stirrups where reinforcement congestion necessitates construction efficiency, and revising torsional strength formulations to integrate the influence of stirrup geometry on load capacity.

These findings underscore the potential benefits of utilizing U-shaped and two-piece enclosed stirrups to enhance the strength, ductility, and energy dissipation capacity of reinforced concrete beams subjected to torsional loading. Their use is particularly advantageous in congested structural zones, such as bridges and high-rise buildings, where placing conventional reinforcement poses significant challenges.

## VII. ACKNOWLEDGMENT

This study was conducted in the Laboratory of the Faculty of Engineering at Ain Shams University, with partial financial support provided by Soada Group for Construction. The author gratefully acknowledges the valuable assistance and technical expertise of the laboratory staff and team throughout the experimental phase of this work. This study has limitations, including a small sample size of only three beams, controlled laboratory conditions without combined loading, and no assessment of long-term durability. Future research should involve larger sample groups, test under more realistic combined loads, and include field validation to enhance applicability of the findings.

## REFERENCES

- [1] MohamedSalih, M. M., & Yousif, A. R. (2022). Effect of type, amount, and configuration of reinforcement in HSC box-girders reinforced with BFRP bars and steel stirrups under torsion-shear-bending. *Ain Shams Engineering Journal*, 13(6), 101787. doi: 10.1016/j.asej.2022.101787.
- [2] Shatarat, N., Hunifat, R., Murad, Y., Katkhuda, H., & Abdel Jaber, M. (2020). Torsional capacity investigation of reinforced concrete beams with different configurations of welded and unwelded transverse reinforcement. *Structural Concrete*, 21(2), 484–500. doi:10.1002/suco.201900054.
- [3] Katkhuda, H. N., Shatarat, N. K., & AL-Rakhameen, A. A. (2019). Improving the Torsional Capacity of Reinforced Concrete Beams with Spiral Reinforcement. *International Journal of Structural and Civil Engineering Research*, 8(2), 113–118. doi:10.18178/ijscer.8.2.113-118.
- [4] Rashidi, M., & Takhtfiroozeh, H. (2017). The Evaluation of Torsional Strength in Reinforced Concrete Beams. *Mechanics, Materials Science & Engineering Journal*, 7. doi:10.13140/RG.2.2.16568.75521.
- [5] Abdel-kareem, A. H., & Salam, A. M. A. El. (2020). Experimental and Analytical Investigation of Reinforced Concrete Beams with Large Web Opening under Pure Torsion. *International Journal of*



- Advanced Engineering, Management and Science, 6(1), 18–33. doi:10.22161/ijaems.61.4.
- [6] Lin F, Zhong Q, Zhang Z, “Flexural behaviour of RC beams reinforced with compressive steel bars and two-piece enclosed stirrups”, Construction and Building Materials, 126:55–65, 2016.
- [7] Lessig NN, “Theoretical and experimental investigation of reinforced concrete elements subjected to combined bending and torsion”, Theory of design and construction of reinforced concrete structures, Moscow, 73–84, 1958.
- [8] Lampert P, Thulimann B, “Torsions Versuch an Stahlbetonbalken (torsion test on reinforced concrete beams)”. Report no. 6502-2, Institution Fuer Baustatik, ETH, Zurich, Switzerland, 1968.
- [9] Collins MP, “Torque-twist characteristics of reinforced concrete beams. Inelastic and nonlinearity in structural concrete”, University of Waterloo Press, Waterloo, Ontario, Canada, pp 211–231, 1973.
- [10] Hsu TT, Mo YL, “Softening of concrete in torsional members-theory and tests”, Journal of the American Concrete Institute, 82(3):290–303, 1985.
- [11] Bernardo LFA, Lopes SMR, “Behavior of concrete beams under torsion – NSC plain and hollow beams”, Materials & Structures, 41(6):1143–1167, 2008.
- [12] Jeng CH, “Unified softened membrane model for torsion in hollow and solid reinforced concrete members: modeling precracking and postcracking behavior”, Journal of Structural Engineering, 141(10): 04014243, 2014.
- [13] ACI Committee 318, 2019. Building code requirements for structural concrete and commentary (ACI 318M-19). American Concrete Institute.
- [14] Behera, U., and Rajagopalan, K. S., 1969, “Two-Piece U-Stirrups in Reinforced Concrete Beams,” ACI Journal Proceedings, V. 66, No. 7, July, pp. 522-524.
- [15] Housing and Building National Research Center (HBRC). Egyptian Code for Design and Construction of Reinforced Concrete Structures (ECP 203-2020), Cairo, Egypt, 2020.

